

High gain Ga₂O₃ solar-blind photodetectors realized via a carrier multiplication process

G. C. Hu,^{1,2} C. X. Shan,^{1,2} Nan Zhang,^{1,2} M. M. Jiang,¹ S. P. Wang,¹ and D. Z. Shen^{1,*}

¹State Key Laboratory of Luminescence and Applications, Changchun Institute of Optics, Fine Mechanics and Physics, Chinese Academy of Sciences, Changchun 130033, China

²University of Chinese Academy of Sciences, Beijing 10049, China

*shancx@ciomp.ac.cn

Abstract: Ga₂O₃ photodetectors with interdigitated electrodes have been designed and fabricated, and the Ga₂O₃ area exposed to illumination acts as the active layer of the photodetector, while the area covered by Au interdigital electrode provide an arena for carrier multiplication. The photodetectors show a maximum responsivity at around 255 nm and a cutoff wavelength of 260 nm, which lies in the solar-blind region. The responsivity of the photodetector reaches 17 A/W when the bias voltage is 20 V, which corresponds to a quantum efficiency of 8228%, amongst the best value ever reported in Ga₂O₃ film based solar-blind photodetectors.

©2015 Optical Society of America

OCIS codes: (040.5160) Photodetectors; (040.7190) Ultraviolet; (160.6000) Semiconductor materials; (310.6845) Thin film devices and applications.

References and links

1. M. Razeghi and A. Rogalski, "Semiconductor ultraviolet detectors," *J. Appl. Phys.* **79**(10), 7433–7473 (1996).
2. G. M. Ali and P. Chakrabarti, "ZnO-based interdigitated MSM and MISIM ultraviolet photodetectors," *J. Phys. D Appl. Phys.* **43**(41), 415103 (2010).
3. W. J. Wang, C. X. Shan, H. Zhu, F. Y. Ma, D. Z. Shen, X. W. Fan, and K. L. Choy, "Metal–insulator–semiconductor–insulator–metal structured titanium dioxide ultraviolet photodetector," *J. Phys. D Appl. Phys.* **43**(4), 045102 (2010).
4. J. Xing, H. Y. Wei, E. J. Guo, and F. Yang, "Highly sensitive fast-response UV photodetectors based on epitaxial TiO₂ films," *J. Phys. D Appl. Phys.* **44**(37), 375104 (2011).
5. J. S. Liu, C. X. Shan, B. H. Li, Z. Z. Zhang, C. L. Yang, D. Z. Shen, and X. W. Fan, "High responsivity ultraviolet photodetector realized via a carrier-trapping process," *Appl. Phys. Lett.* **97**(25), 251102 (2010).
6. H. Zhu, C. X. Shan, L. K. Wang, J. Zheng, J. Y. Zhang, B. Yao, and D. Z. Shen, "Metal–oxide–semiconductor-structured MgZnO ultraviolet photodetector with high internal gain," *J. Phys. Chem. C* **114**(15), 7169–7172 (2010).
7. E. Munoz, "(Al,In,Ga)N-based photodetectors: some materials issues," *Phys. Status Solidi B* **244**(8), 2859–2877 (2007).
8. T. Takagi, H. Tanaka, S. Fujita, and S. Fujita, "Molecular beam epitaxy of high magnesium content single-phase wurzite Mg_xZn_{1-x}O alloys (x < 0.5) and their application to solar-blind region photodetectors," *Jpn. J. Appl. Phys.* **42**(4B), L401 (2003).
9. K. Koike, K. Hama, I. Nakashima, G. Takada, K. Ogata, S. Sasa, M. Inoue, and M. Yano, "Molecular beam epitaxial growth of wide bandgap ZnMgO alloy films on (111)-oriented Si substrate toward UV-detector applications," *J. Cryst. Growth* **278**(1–4), 288–292 (2005).
10. M. Liao, Y. Koide, and J. Alvarez, "Single Schottky-barrier photodiode with interdigitated-finger geometry: Application to diamond," *Appl. Phys. Lett.* **90**(12), 123507 (2007).
11. R. Zou, Z. Zhang, Q. Liu, J. Hu, L. Sang, M. Liao, and W. Zhang, "High detectivity solar-blind high-temperature deep-ultraviolet photodetector based on multi-layered (100) facet-oriented β-Ga₂O₃ nanobelts," *Small* **10**(9), 1848–1856 (2014).
12. Z. Ji, J. Du, J. Fan, and W. Wang, "Gallium oxide films for filter and solar-blind UV detector," *Opt. Mater.* **28**(4), 415–417 (2006).
13. Y. Kokubun, K. Miura, F. Endo, and S. Nakagomi, "Sol-gel prepared β-Ga₂O₃ thin films for ultraviolet photodetectors," *Appl. Phys. Lett.* **90**(3), 031912 (2007).
14. T. Oshima, T. Okuno, and S. Fujita, "Ga₂O₃ thin film growth on c-plane sapphire substrates by molecular beam epitaxy for deep-ultraviolet photodetectors," *Jpn. J. Appl. Phys.* **46**(11), 7217–7220 (2007).
15. P. Feng, J. Y. Zhang, Q. H. Li, and T. H. Wang, "Individual β-Ga₂O₃ nanowires as solar-blind photodetectors," *Appl. Phys. Lett.* **88**(15), 153107 (2006).
16. T. Oshima, T. Okuno, N. Arai, N. Suzuki, S. Ohira, and S. Fujita, "vertical solar-blind deep-ultraviolet schottky photodetectors based on β-Ga₂O₃ substrates," *Appl. Phys. Express* **1**(1), 011202 (2008).

17. R. Suzuki, S. Nakagomi, Y. Kokubun, N. Arai, and S. Ohira, "Enhancement of responsivity in solar-blind β -Ga₂O₃ photodiodes with a Au Schottky contact fabricated on single crystal substrates by annealing," *Appl. Phys. Lett.* **94**(22), 222102 (2009).
18. R. McClintock, J. L. Pau, K. Minder, C. Bayram, P. Kung, and M. Razeghi, "Hole-initiated multiplication in back-illuminated GaN avalanche photodiodes," *Appl. Phys. Lett.* **90**(14), 141112 (2007).
19. X. G. Bai, H. D. Liu, D. C. McIntosh, and J. C. Campbell, "High-detectivity and high-single-photon-detection-efficiency 4H-SiC avalanche photodiodes," *IEEE J. Quantum Electron.* **45**(3), 300–303 (2009).
20. J. L. Pau, R. McClintock, M. Razeghi, and D. Silversmith, "Back-illuminated separate absorption and multiplication GaN avalanche photodiodes," *Appl. Phys. Lett.* **92**(10), 101120 (2008).
21. F. Xie, H. Lu, D. J. Chen, X. Q. Xiu, H. Zhao, R. Zhang, and Y. D. Zheng, "Included in your digital subscription metal–semiconductor–metal ultraviolet avalanche photodiodes fabricated on bulk GaN substrate," *IEEE Electron Device Lett.* **32**(9), 1260–1262 (2011).
22. J. C. Carrano, D. J. H. Lambert, C. J. Eiting, C. J. Collins, T. Li, S. Wang, B. Yang, A. L. Beck, R. D. Dupuis, and J. C. Campbell, "GaN avalanche photodiodes," *Appl. Phys. Lett.* **76**(7), 924 (2000).
23. C. Bayram, J. L. Pau, R. McClintock, and M. Razeghi, "Performance enhancement of GaN ultraviolet avalanche photodiodes with p-type δ -doping," *Appl. Phys. Lett.* **92**(24), 241103 (2008).
24. K. Minder, J. L. Pau, R. McClintock, P. Kung, C. Bayram, M. Razeghi, and D. Silversmith, "Scaling in back-illuminated GaN avalanche photodiodes," *Appl. Phys. Lett.* **91**(7), 073513 (2007).
25. C. Bayram, J. L. Pau, R. McClintock, M. Razeghi, M. P. Ulmer, and D. Silversmith, "High quantum efficiency back-illuminated GaN avalanche photodiodes," *Appl. Phys. Lett.* **93**(21), 211107 (2008).
26. J. Yu, C. X. Shan, J. S. Liu, X. W. Zhang, B. H. Li, and D. Z. Shen, "MgZnO avalanche photodetectors realized in Schottky structures," *Phys. Status Solidi Rapid Res. Lett.* **7**(6), 425–428 (2013).
27. J. Yu, C. X. Shan, X. M. Huang, X. W. Zhang, S. P. Wang, and D. Z. Shen, "ZnO-based ultraviolet avalanche photodetectors," *J. Phys. D Appl. Phys.* **46**(30), 305105 (2013).
28. A. Axelevitch, B. Gorenstein, and G. Golan, "Investigation of optical transmission in thin metal films," *Physics Procedia* **32**, 1–13 (2012).
29. D. Y. Guo, Z. P. Wu, P. G. Li, Y. H. An, H. Liu, X. C. Guo, H. Yan, G. F. Wang, C. L. Sun, L. H. Li, and W. H. Tang, "Fabrication of β -Ga₂O₃ thin films and solar-blind photodetectors by laser MBE technology," *Opt. Mater. Express* **4**(5), 1067–1076 (2014).
30. Y. Kokubun, K. Miura, F. Endo, and S. Nakagomi, "Sol-gel prepared β -Ga₂O₃ thin films for ultraviolet photodetectors," *Appl. Phys. Lett.* **90**(3), 031912 (2007).
31. S. M. Sze, *Physics of Semiconductor Devices*, 2nd ed. (John Wiley, 1981).
32. X. Gong, M. Tong, Y. Xia, W. Cai, J. S. Moon, Y. Cao, G. Yu, C. L. Shieh, B. Nilsson, and A. J. Heeger, "High-detectivity polymer photodetectors with spectral response from 300 nm to 1450 nm," *Science* **325**(5948), 1665–1667 (2009).
33. M. D. Sing, W. S. Liang, R. H. Horng, P. Ravadgar, T. Y. Wang, and H. Y. Lee, "Growth and characterization of Ga₂O₃ on sapphire substrates for UV sensor applications," *Proc. SPIE* **8263**, 826317 (2012).
34. P. Guo, J. Xiong, X. H. Zhao, T. Sheng, C. Yue, B. Tao, and X. Z. Liu, "Growth characteristics and device properties of MOD derived β -Ga₂O₃ films," *J. Mater. Sci. Mater. Electron.* **25**(8), 3629–3632 (2014).
35. S. Nakagomi, T. Momo, S. Takahashi, and Y. Kokubun, "Deep ultraviolet photodiodes based on Ga₂O₃/SiC heterojunction," *Appl. Phys. Lett.* **103**(7), 072105 (2013).
36. Y. Kokubun, K. Miura, F. Endo, and S. Nakagomi, "Sol-gel prepared β -Ga₂O₃ thin films for ultraviolet photodetectors," *Appl. Phys. Lett.* **90**(3), 031912 (2007).
37. L. Esaki, "New phenomenon in narrow germanium *p-n* junctions," *Phys. Rev.* **109**(2), 603–604 (1958).
38. T. D. Moustakkas and M. Misra, "Origin of the high photoconductive gain in AlGa_N films," *Proc. SPIE* **6766**, 67660C (2007).
39. S. M. Sze, D. J. Coleman, Jr., and A. Loya, "Current transport in metal-semiconductor-metal (MSM) structures," *Solid-State Electron.* **14**(12), 1209–1218 (1971).
40. H. Zhu, C. X. Shan, J. Y. Zhang, Z. Z. Zhang, B. H. Li, D. X. Zhao, B. Yao, D. Z. Shen, X. W. Fan, Z. K. Tang, X. Hou, and K. L. Choy, "Low-threshold electrically pumped random lasers," *Adv. Mater.* **22**(16), 1877–1881 (2010).
41. X. Y. Ma, P. L. Chen, D. S. Li, Y. Y. Zhang, and D. R. Yang, "Electrically pumped ZnO film ultraviolet random lasers on silicon substrate," *Appl. Phys. Lett.* **91**(25), 251109 (2007).
42. H. Zhu, C. X. Shan, B. H. Li, Z. Z. Zhang, D. Z. Shen, and K. L. Choy, "Low-threshold electrically pumped ultraviolet laser diode," *J. Mater. Chem.* **21**(9), 2848–2851 (2011).

1. Introduction

Solar-blind photodetectors that can response to photons with wavelength shorter than 280 nm have attracted much attention in recent years for their versatile potential applications in missile warning, flame sensing, space communications, etc [1–6]. To date, wide bandgap semiconductors, such as AlGa_N, MgZnO, and diamond, have been considered as promising candidates for solar-blind photodetectors [7–10]. Besides the above mentioned candidates, gallium oxide (Ga₂O₃) has also attracted much attention for its wide bandgap (4.8 eV), which lies sharply in the solar-blind spectrum region, and its high chemical and thermal stability, which is favorable for robust devices that can work in harsh environment [11]. Actually,

many reports on Ga₂O₃ solar-blind photodetectors have appeared in recent years. Ga₂O₃ thin films [12–14] nanowires [15] and single crystals [16,17] have been employed as the active layer for such photodetectors, and many types of Ga₂O₃ photodetectors, for example photoconductive type [12], Schottky structure [17], metal-semiconductor-metal structures [17], have been reported so far. How to realize high gain is one of the key issues for the future applications of Ga₂O₃ solar-blind photodetectors. To this end, some methods have been employed, and a typical one is to construct a photoconductive structure, in which the responsivity of the photodetector can be enhanced greatly with holes trapped by the surface states at the metal-semiconductor surface.⁵ Nevertheless, such a process will degrade the response time of the photodetectors drastically, which restricts the application of such photodetectors in many areas. It is accepted that carrier multiplication will occur via an impact ionization process under relatively large bias, and we have shown that if such a carrier multiplication can be employed in a photodetector, the responsivity of the photodetector will be enhanced greatly [18–26]. However, such a strategy has only been applied in GaN and ZnO based ultraviolet photodetectors [21,27], while none report about this kind of mechanism in Ga₂O₃ photodetectors can be found up to date.

In this paper, Au/Ga₂O₃/Au structures with interdigital electrodes have been designed and constructed. The Ga₂O₃ area exposed to illumination acts as the active layer of the photodetector, while the area covered by Au interdigital electrode provides an arena for carrier multiplication that is responsible for the gain in the Ga₂O₃ photodetectors. The responsivity of the Ga₂O₃ photodetector can reach 17 A/W at 20 V bias, which corresponds to a quantum efficiency of 8228%, comparable to the best value ever reported in Ga₂O₃ film based photodetectors.

2. Experiments

The Ga₂O₃ films employed as the active layer of the photodetectors were grown on *a*-plane sapphire substrate by metal-organic chemical vapor deposition (MOCVD) technique. Oxygen (O₂) and triethylgallium (TEGa) were employed as the precursor for the growth, and nitrogen (7 N) was used as the carrier gas. Briefly, the growth was carried out at a substrate temperature of 850 °C and a chamber pressure of around 500 Torr, and the mole ratio of TEGa/O₂ that were introduced to the growth chamber during the growth process was around 300. The structural properties of the films were evaluated by an x-ray diffractometer with Cu K α line (0.154 nm) as the radiation source. The absorption and transmission spectra of the films were recorded in a Shimadzu UV-3101PC scanning spectrophotometer. As for the fabrication of the photodetector, standard photolithography and lift-off techniques are used to define the interdigitated electrodes, which are based on a 200 nm Au metal stack. The fingers of the interdigitated electrodes are 10 μ m in width and 500 μ m in length with a spacing of 10 μ m. The effective device area of the photodetector is 400 \times 500 μ m². Note that the Ga₂O₃ area underneath the Au electrode will not be illuminated by the UV illumination because of the Au electrodes covering [28]. The electrical characteristics of the photodetectors were measured in an Agilent B1500A Semiconductor Device Analyzer. The photoresponse of the photodetectors was measured in a SPEX scanning monochromator employing a 150 W Xe lamp as the illumination source. The spectrum of the Xe lamp can cover from 200 nm to over 1000 nm, and the responsivity spectrum is obtained by measuring the photocurrent (calibrated with a standard Si photodiode) under the illumination of the Xe lamp spectrum from 200 nm to 500 nm using the scanning monochromator.

3. Results and discussion

The typical absorption spectra of the Ga₂O₃ films are shown in Fig. 1(a). It can be seen that the films have a strong absorption in the solar-blind spectrum region with a sharp absorption edge at around 254 nm, while they are almost transparent in the visible region. The above characters are favorable for their application in high-performance solar-blind photodetectors. For β -Ga₂O₃ with a direct bandgap, the absorption follows Eq. (1):

$$(\alpha hv)^2 = B(hv - E_g) \quad (1)$$

Where α is the absorption coefficient, hv is the energy of the incident photon, B is a constant, and E_g is the band gap. The optical absorption coefficient, α , of the film is evaluated using the relation:

$$\alpha = \left[\frac{1}{d} \right] \ln(10^A) \quad (2)$$

Where A is the absorbance, and d is the film thickness. Eq. (1) can be simplified as

$$A^2 = \frac{Bd^2}{h^2\nu^2}(hv - E_g) \quad (3)$$

The bandgap is determined by extrapolating the linear region of the plot A^2 vs hv and taking the intercept on the hv -axis. The derived bandgap is ~ 4.98 eV as shown in the inset of Fig. 1(a). The above value is in rough agreement with the bandgap of Ga_2O_3 reported in literature (4.8 eV) [14]. Figure 1(b) illustrates the x-ray diffraction (XRD) pattern of the Ga_2O_3 films. Besides the diffraction from the sapphire substrate, two peaks can be observed. The peak located at 18.78° can be indexed to the diffraction from $(\bar{1}02)$ facet [29], while the one at 34.97° to that from the (111) facet of $\beta\text{-Ga}_2\text{O}_3$ [30]. The XRD data reveal that the Ga_2O_3 films are crystallized in monoclinic structure.

Figure 2 shows the current–voltage (I – V) characteristics of the $\text{Au}/\text{Ga}_2\text{O}_3/\text{Au}$ structure measured under dark and 255 nm light illumination conditions and the optical power density of the illumination source is $0.12 \mu\text{W}/\text{mm}^2$. Note that the dark current of the device is about 6.2×10^{-10} A when the bias is 20 V, while under the illumination of the 255 nm light, the current has been increased to 2.9×10^{-6} A, that is the current has been enhanced by over three orders. The above phenomenon means that the resistance of the Ga_2O_3 films has been decreased significantly under the illumination of the 255 nm light. The significant increase of the current under illumination promises that high performance photodetectors may be realized from the Ga_2O_3 films.

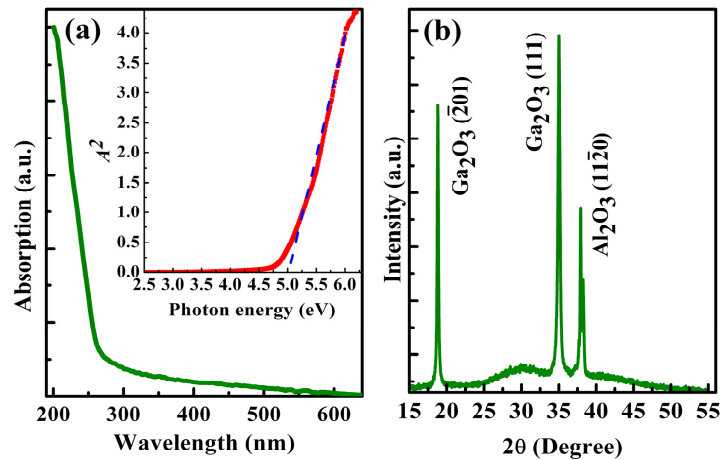


Fig. 1. Room temperature absorption spectrum of the Ga_2O_3 films, and the inset shows A^2 versus hv of the $\beta\text{-Ga}_2\text{O}_3$ thin films (a) and the XRD pattern of the $\beta\text{-Ga}_2\text{O}_3$ films (b).

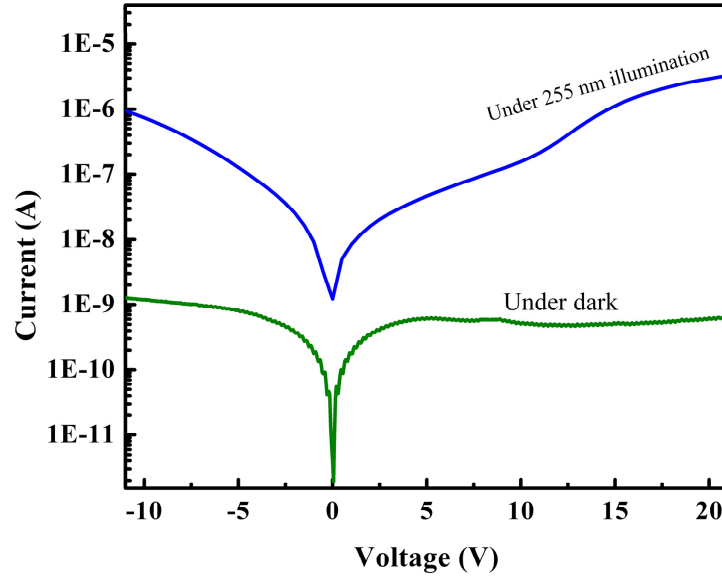


Fig. 2. I - V characteristics of the Ga_2O_3 photodetector measured under dark and 255 nm light illumination conditions.

The typical photoresponse spectrum of the $\text{Au}/\text{Ga}_2\text{O}_3/\text{Au}$ structured photodetector is shown in Fig. 3. The spectrum shows a predominant peak at around 255 nm, and the cutoff wavelength of the photodetector occurs at ~ 260 nm. The UV-to-visible rejection ratio that is defined as the responsivity ratio at 255 nm and that at 450 nm of around 8.5×10^6 is achieved in the photodetector. The inset of Fig. 3 shows the maximum responsivity of the photodetector as a function of the applied bias. One can see in the low bias range, the responsivity increases gradually with the bias, but it increases abruptly when the bias is over 6 V. The quantum efficiency of the photodetector as a function of the applied bias is also shown in the inset of Fig. 3, in which the external quantum efficiency η is given by the following formula [31]:

$$\eta = \frac{hcR_\lambda}{(e\lambda)} \quad (4)$$

Where R_λ is the responsivity of a photodetector, h is Planck's constant, c is the velocity of light, e is the basic electron charge, and λ is the incident light wavelength. One can see that the quantum efficiency exceeds 100% when the bias is larger than 8 V and reaches 8228% at 20 V, which means that there is large gain in the photodetector. The detectivity (D^*) of a photodetector can be determined by the following expression [32]:

$$D^* = \frac{R}{\sqrt{2qJ_d}} \quad (5)$$

where R is the responsivity of the photodetector, q is the elemental charge and J_d is the dark current density. Considering that $R = 17$ A/W, $J_d = 1.85 \times 10^{-6}$ A/cm², one can deduce that the detectivity of the photodetector $D^* = 7.0 \times 10^{12}$ Jones from Eq. (5). Table 1 shows the comparison of the responsivity and external quantum efficiency of the reported $\beta\text{-Ga}_2\text{O}_3$ film based photodetectors, one can see from the table that the responsivity reported in this paper is amongst the best value ever reported for Ga_2O_3 film based photodetectors.

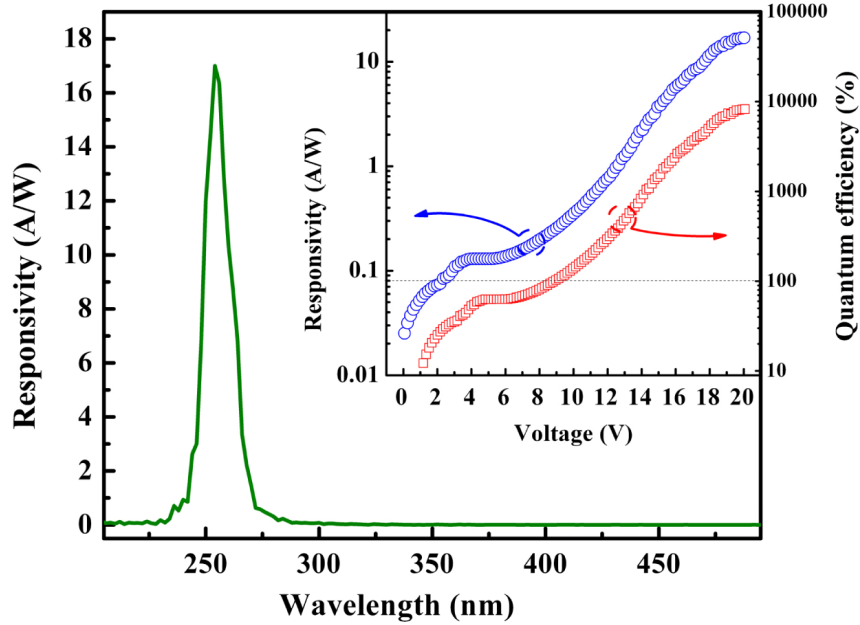


Fig. 3. A typical photoresponse spectrum of the photodetector at 20 V, and the inset shows the maximum responsivity and quantum efficiency of the photodetector as a function of the applied bias.

The electric potential of the Au/Ga₂O₃/Au structure under 20 V is simulated by COMSOL Multiphysics software. There are 20 pairs of interdigital electrodes in the device, and for the simulation, one pair of the interdigital electrode is employed as the example. The width of the fingers is 10 μm, and the length is 500 μm, and the spacing between the adjacent fingers is 10 μm. The resistance of the Ga₂O₃ films is in the order of 10 GΩ under dark conditions, while it is around 10 MΩ under the illumination of the 255 nm light. The parameters used for the simulation is as follows: bandgap: 4.98 eV; Mobility: 300 cm²/Vs; Relative permittivity: 10; Thermal conductivity: 0.14 W/cmK. Figure 4(a) shows the dark condition. One can see that there is no intersection between electric field lines of the positive pole and the negative pole, which means the Ga₂O₃ is totally insulating under dark conditions. Figure 4(b) shows the condition with 255 nm light illumination. One can see that the electric potential is mainly focused on the Ga₂O₃ surface and the density of electric potential line beneath the positive pole is the highest, which means that there exists relatively high electric field, and carrier multiplication prefers to occur there.

Table 1. Comparison of the photoresponse parameters among β-Ga₂O₃ film based photodetectors.

Photodetectors	Responsivity	External quantum efficiency	Reference
β-Ga ₂ O ₃ thin film	20.1 A/W	–	[33]
β-Ga ₂ O ₃ thin film	0.76 A/W	–	[34]
β-Ga ₂ O ₃ thin film	0.07 A/W	–	[35]
β-Ga ₂ O ₃ thin film	8 × 10 ⁻⁵ A/W	–	[36]
β-Ga ₂ O ₃ thin film	17 A/W	8228%	This work

There are three mainly mechanisms, that is photoconductive gain, Zener tunneling, and avalanche multiplication, may contribute to the high responsivity and quantum efficiency of a photodetector. As for Zener tunneling, it usually occurs in highly doped semiconductors under small bias [37], while in our case, the Ga₂O₃ films have not been doped at all, so the high responsivity and quantum efficiency caused by Zener tunneling may not exist in the

Au/Ga₂O₃/Au structure. With reference to the photoconductive gain, the responsivity tends to saturate at elevated bias [31]. However, from the inset of Fig. 3, one can see that the responsivity of the photodetector increases gradually and then abruptly with the applied

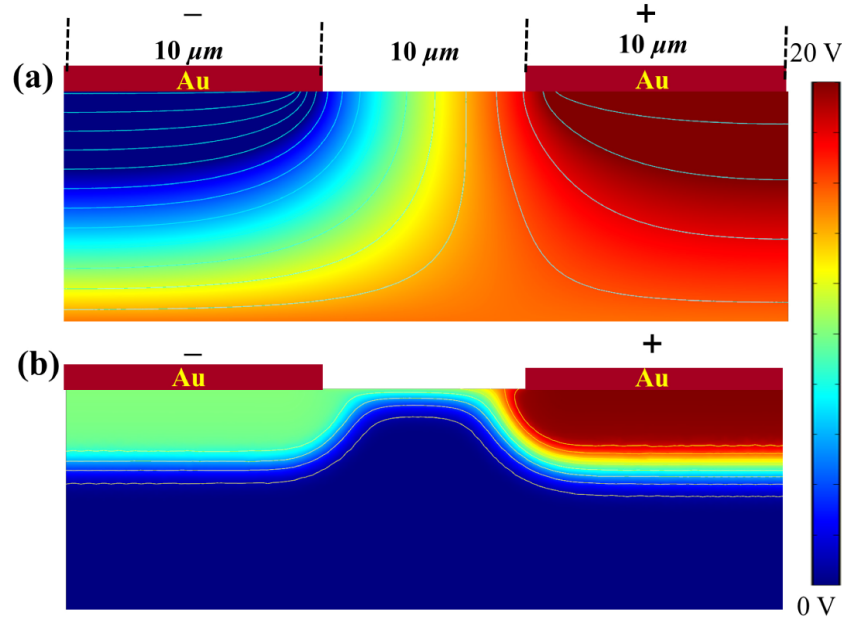


Fig. 4. Simulated electric potential profile of the Au/Ga₂O₃/Au structure under 20 V with (a) and without (b) 255 nm light illumination conditions.

voltage, indicating that the photoconductive gain cannot be the dominant factor in this case. Thus it is speculated that the gain in the Ga₂O₃ solar-blind photodetector may come from the carrier multiplication, which can be understood as follows: When light is illuminated onto the Au/Ga₂O₃/Au structure, because of the interdigitated structure, only the area without the electrode is exposed to the UV illumination, while the area underneath the Au electrode cannot be illuminated, the situation of which is shown schematically in Fig. 5(a). It is known that under the illumination of UV light, the photons with their energy larger than the bandgap of Ga₂O₃ will be absorbed, and the electrons in the valence band of Ga₂O₃ will be excited to its conduction band, and holes are left in the valence band. This is the generation process of photogenerated electrons and holes. One can see from the I - V curve shown in Fig. 2 that upon the illumination of UV light, the resistivity of the Ga₂O₃ will be decreased significantly. That is, the resistivity of the area under the exposure of the UV illumination will be decreased greatly, while that of the area underneath the Au electrode is still large. Then when the bias voltage is applied onto the structure, most of the bias will be applied onto the area underneath the Au electrode, and the electric field in such area will be very large, as the situation shown in Fig. 4. Then when the photogenerated carriers are drifted into this area, the carriers will be accelerated greatly, and the accelerated carriers may impact with the lattice of the Ga₂O₃ to release their kinetic energy and generate additional electrons and holes. The generated electrons and holes will again gain much kinetic energy from the electric field and generate more additional electrons and holes. In this way, carrier multiplication occurs [38–42], and the number of the carriers that can be collected by the Au interdigital electrode will be increased greatly, then the great gain of the photodetectors will be achieved, as shown in Fig. 5(b).

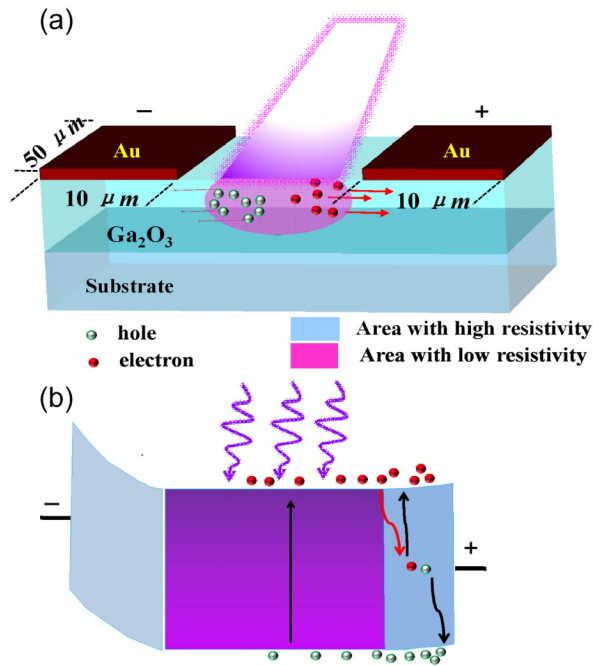


Fig. 5. (a) Side view of the Au/Ga₂O₃/Au structure under 255 nm illumination and (b) Schematic bandgap alignment of the Ga₂O₃ structure under reverse bias.

4. Conclusion

In summary, Ga₂O₃ solar-blind photodetectors have been fabricated from Au/Ga₂O₃/Au structures, and the photodetector exhibits a responsivity of 17 A/W, a UV-to-visible rejection ratio with 8.5×10^6 , and a quantum efficiency of around 8228% at 20 V bias, which are comparable to the best results in Ga₂O₃ film based photodetectors. The optical gain in the photodetector has been attributed to come from the carrier multiplication occurred in the Ga₂O₃ area cover by the interdigital Au electrode. The results reported in this paper may provide a promising route to high-performance Ga₂O₃ solar-blind photodetectors.

Acknowledgments

This work is financially supported by the National Basic Research Program of China (2011CB302006), the National Science Foundation for Distinguished Young Scholars of China (61425021), the Natural Science Foundation of China (11134009, 11374296, 61376054, and 61177040), and the Science and Technology Developing Project of Jilin Province (20111801).